Proc. NIPR Symp. Upper Atmos. Phys., **11**, 36–54, 1998

ALTITUDE PROFILE OF ELECTRON DENSITY AND OXYGEN GREEN LINE IN ACTIVE AURORAL ARCS BASED ON ELECTRON DIFFERENTIAL NUMBER FLUX OBSERVED BY SOUNDING ROCKET

Kunizo ONDA[1], Masaki EJIRI[2], Yukikazu ITIKAWA[3] and Hiroshi MIYAOKA[2]

[1]*Faculty of Industrial Science and Technology, Science University of Tokyo, Oshamambe, Yamakoshi-gun, Hokkaido 049-3514*
[2]*National Institute of Polar Research, 9–10, Kaga 1-chome, Itabashi-ku, Tokyo 173-8515*
[3]*Institute of Space and Astronautical Science, 1–1, Yoshinodai 3-chome, Sagamihara 229-8510*

Abstract: The Monte Carlo method was applied to investigate electron auroras observed by the sounding rocket S-310JA-8, which was launched on April 4, 1984 from Syowa Station in Antarctica of the invariant latitude 66.14°S and the geomagnetic longitude 70.98°. The number density of the atmosphere, in which constituent elements were assumed to be N_2, O and O_2, and temperatures were estimated by the MSIS-86 model for the aurora observed there. A downward electron differential number flux was measured at the altitude of 200 km, from which electrons were injected downward into the upper atmosphere. An initial electron energy E_0 is investigated in the range from 100 eV to 18 keV. An initial pitch angle was assumed to be uniformly distributed in the range of $[0, \pi/2]$.

Ionization rates of N_2, O and O_2 were calculated as a function of an altitude, the initial pitch angle, and the initial electron energy. The total ionization rate obtained by summing up individual ionization rate was considered to be a production rate of thermal electrons. A loss rate of thermal electrons was estimated by using an electron density and an effective recombination rate. Under the assumption of local equilibrium of ionization and recombination, the height profile of electron density was deduced and compared with the observed one.

The height profile of an emission rate was also investigated for the oxygen green line. The emission rate calculated as contribution from the electron impact was compared with the one produced by the collision process $N_2(A^3\Sigma_u^+) + O(^3P)$, and it was made clear that the latter collision process was more efficient to excite oxygen atoms from $O(^3P)$ to $O(^1S)$ than the electron impact in the wide range of electron energy observed by the sounding rocket.

1. Introduction

It is highly desirable that experimentalists and theoreticians make plans for coordinated observations and analyses of some auroral events, carry out such plans, and collaborate with each other for understanding deeply the physics of these natural events. But, it is not easy to realize these projects, because auroras are sporadic events and rocket experiments take a long span of time for campaign setup. Furthermore, it is not established yet that any theoretical method is applicable to analyzing properly observed results and is useful for understanding them. Therefore, it is interesting to clarify whether or not any theoretical approach succeeds in representing collision

processes between precipitating electrons and constituent elements of the upper atmosphere and predicts the rates of excitation and ionization of atmospheric constituents and resulting emission rates in electron auroras.

In the past, REES (1963), BANKS *et al.* (1974), STRICKLAND *et al.* (1976), SOLOMON *et al.* (1988), and LINK (1992) studied electron transport and energy deposition of auroral electrons, and some review papers related to electron auroras were written by REES (1969), REES and ROBLE (1975), TORR and TORR (1982), REES (1987), and SOLOMON (1991). Specifically, BERGER *et al.* (1970), CICERONE and BOWHILL (1971), JACKMAN and GREEN (1979), and very recently SOLOMON (1993) and SERGIENKO and IVANOV (1993) applied the Monte Carlo method to electron transport problems related to electron auroras. Most of them employed empirically fitted formulas (JACKMAN and GREEN, 1979; YUROVA and IVANOV, 1989) for collision cross sections of electrons scattered from N_2, O, and O_2 gases.

The sounding rocket S-310JA-8 was launched from Syowa Station in Antarctica of the invariant latitude 66.14°S and the geomagnetic longitude 70.98° at the magnetic local time being nearly equal to the universal time 1927:01(UT) on April 4, 1984 toward active auroral arcs at a substorm expansion phase. An upper hybrid resonance in a plasma was detected by a frequency-sweep impedance probe, from which the electron density of the plasma was deduced (see OYA, 1965; EJIRI and OBAYASHI, 1970). A quadrispherical electrostatic spectrometer measured an energy spectrum of electrons in the range from 16 eV to 14.4 keV. EJIRI (1988) and EJIRI *et al.* (1988a, b, c) reported observational results in detail.

We calculated in a previous study the photoemission rate for the first negative band system of N_2^+ at λ 427.8 nm by using the Monte Carlo method. The absolute intensity of this emission was determined by combining our numerical results for single electron with the downward electron differential number flux, which is simply denoted as the electron differential flux hereafter. This theoretical absolute intensity reasonably agreed with the experimental one as reported by ONDA *et al.* (1997). This confirms the applicability of the Monte Carlo method to the collision processes in electron auroras. In order to further make clear quantitative accuracy of the Monte Carlo method, we aimed in this study at estimating number density of thermal electrons measured simultaneously at the event of the active auroral arcs by the sounding rocket S-310JA-8.

The next section briefly describes the outline of the Monte Carlo method (see ONDA *et al.*, 1992, in detail). Ionization rates of N_2, O, and O_2 were calculated and a loss rate of thermal electrons was estimated by using the electron density and an effective recombination coefficient. A height distribution of electron density was deduced by the consideration based on the assumption that the production and loss of thermal electrons were locally in equilibrium. These numerical results are presented and discussed in Sections 3.1 and 3.2.

The rates of production and emission of oxygen green line were also derived from the results of the Monte Carlo method and are presented in Section 3.3. In addition to the electron impact, the rate of production of the oxygen green line was also estimated by taking into account collision process of $N_2(A^3\Sigma_u^+)+O(^3P)$. After that, the height profile of the green line emission rate was compared with the one of the first

negative band system of N_2^+ at λ 427.8 nm. These results give us some ideas on the absolute value of emission rate of the oxygen green line relative to that of N_2^+ at λ 427.8 nm in active auroral arcs (OKAMURA and EJIRI, 1992).

Concluding remarks are stated in the final Section 4.

2. Calculations

We regarded the geomagnetic lines of force as approximately straight in the altitude range from 80 to 200 km, and took the z axis of our coordinate system along the line of force. On the assumption that only the geomagnetic field causes the Lorentz force on an electron and any electric field has no effect on the motion of electrons, we determined the motion of the electron between collisions with the atmospheric particles by solving the classical equation of motion. SI units were used throughout this paper unless otherwise stated.

The details of the Monte Carlo calculation were described in a previous paper by ONDA *et al.* (1992).

Atmospheric number densities and temperatures were represented by the MSIS-86 model (HEDIN, 1983, 1987) for aurora observed at the invariant latitude 66.14° and the geomagnetic longitude 70.98° on April 4, 1984. The number densities of N_2, O and O_2, which were assumed as the sole constituent elements of the atmosphere, were shown in Fig. 1 of the previous paper of ONDA *et al.* (1997). The following parameters were adopted in this study: $T_{ex}=1170.28$°K; F107=129.0; F107A=125.1; and Ap=84.0.

We took into account a momentum-transfer in the elastic collision between the electron and N_2, O, or O_2. The corresponding energy loss was given by $\Delta E=(2m/M_j)(1-\cos\omega)E_i$, where m is the mass of the electron, M_j is that of the jth atmospheric particle, ω is the scattering angle, and E_i is the energy of the electron before the collision.

Excitation of discrete levels and ionization with or without excitation of residual ions were considered for each neutral component of the atmosphere. The electron energy after an inelastic collision was given by $E_f=E_i-\Delta E$, where ΔE is the energy loss in the inelastic collision. The energy loss for an ionizing collision is the sum of the relevant ionization energy and the kinetic energy of the secondary electron. Three electronic states of N_2^+ were distinguished in ionizing collisions of N_2. However, only the ground state was considered for the ions of O and O_2. An approximate analytic expression (OPAL *et al.*, 1971, 1972) for the energy distribution of secondary-electrons was employed for N_2 and O_2. No experimental data are available for the energy distribution of secondary-electrons of atomic oxygen. Therefore, the same analytic form of the energy distribution as that for O_2 was used for atomic oxygen. The number of states taken into account in this work is 17 for N_2, 12 for O, and 10 for O_2 (see ONDA *et al.*, 1992, in detail). The data on collision cross sections summarized by ITIKAWA *et al.* (1986, 1989) and by ITIKAWA and ICHIMURA (1990) were employed in this work as those for electrons scattered from N_2, O, and O_2. Experimental values determined by DOERING and GULCICEK (1989) and DOERING (1992) were considered partly for the excitation cross sections for producing $O(^1D)$ and $O(^1S)$.

The energy loss of the precipitating electrons due to collisions with ambient iono-

spheric electrons was estimated to be negligible (see ONDA *et al.*, 1997).

3. Results and Discussion

An IGRF 90 model was employed to estimate the geomagnetic flux intensity. The resulting values were 40274 nT at an altitude of 250 km, 41070 nT at 200 km, and 42723 nT at 100 km at 1927:01 (UT) on April 4, 1984 at Syowa Station. It was found by ONDA *et al.* (1997) that the excitation and ionization rates were almost insensitive to the magnitude of the magnetic flux density in the range of 30000–50000 nT. Thus, we took the magnetic flux density to be 43000 nT in this study.

In our calculations, the angle β between the local line of force and the vertical was set to be $\beta=25^\circ$ (the declination of the geomagnetic field line is about -64°), and electrons were started at an altitude of $h_0=200$ km (the observational electron spectrum was given at this altitude) downward into the atmosphere. We investigated the energy of precipitating electrons in the range of $E_0=0.1$–18 keV. If the electron energy falls below 2 eV, we stopped tracing of the electrons. A pitch angle α_0 was taken in the range of $\alpha_0=0$–90°. As was shown by ONDA *et al.* (1997), results for $\alpha_0=90^\circ$ will be safely replaced by those for $\alpha_0=80^\circ$.

3.1. Dependence of ionization rates on initial electron pitch angle and energy

The atmospheric constituents N_2, O, and O_2 were ionized through collisions with precipitating electrons and the secondary electrons produced by the ionization. Ionization rates of N_2, O, and O_2 were calculated at the initial electron energies of $E_0=0.1$–18 keV. A height distribution of these ionization rates is presented in Fig. 1a for the initial electron pitch angle $\alpha_0=0^\circ$ and energy $E_0=1$ keV. The total ionization rate is defined here as the sum of the individual ionization rate of N_2, O, and O_2. In Fig. 1b, the result for $\alpha_0=80^\circ$ and $E_0=1$ keV is shown. These ionization rates of N_2, O, and O_2 at $E_0=1$ keV were about 68%, 20%, and 12%, respectively, as a percentage of the total ionization rate, and about 75%, 6%, and 19%, respectively, at $E_0=5$ keV. The results for $E_0=10$ keV are shown in Figs. 2a and 2b for $\alpha_0=0^\circ$ and 80°, respectively. The contribution to the total ionization rate from N_2, O, and O_2 at $E_0=10$ keV was about 76%, 3%, and 21%, respectively. In Figs. 3a and 3b, the results at $E_0=15$ keV are shown for $\alpha_0=0^\circ$ and 80°, respectively. The ionization rates of N_2, O, and O_2 at $E_0=15$ keV are about 77%, 1%, and 22%, respectively, as a percentage of the total ionization rate. The contribution to the ionization rate comes less from oxygen atoms, and more from N_2 molecules as the initial energy of electrons increases. It is easily understandable, because electrons can deeply penetrate into the atmosphere with increasing the initial energy.

The results for $\alpha_0=30^\circ$ and 60° were similar to those for $\alpha_0=0^\circ$ at almost all the initial electron energies considered here. At a height above 140 km, the ionization rate of O atoms was larger than that of O_2 molecules irrespective of the initial electron energy.

Dependence of the total ionization rate on pitch angles is shown in Figs. 4a–4d at the initial electron energies of $E_0=1$, 5, 10, and 15 keV, respectively. As can be understood from these figures, the main contribution to the ionization rate comes from the initial electron energy above about $E_0=5$ keV. It is worth mentioning that the peak

height of the total ionization rate decreased to about 100 km with increasing the initial energy of electrons.

3.2. Height profile of thermal electron density

The sounding rocket experiment was carried out at Syowa Station in Antarctica, on April 4, 1984, in order to investigate the physical causality between the precipitating auroral particles and the resultant photo-emission rates or an ionization rate. The following scientific payloads were installed: the visible auroral TV camera (VAT) to

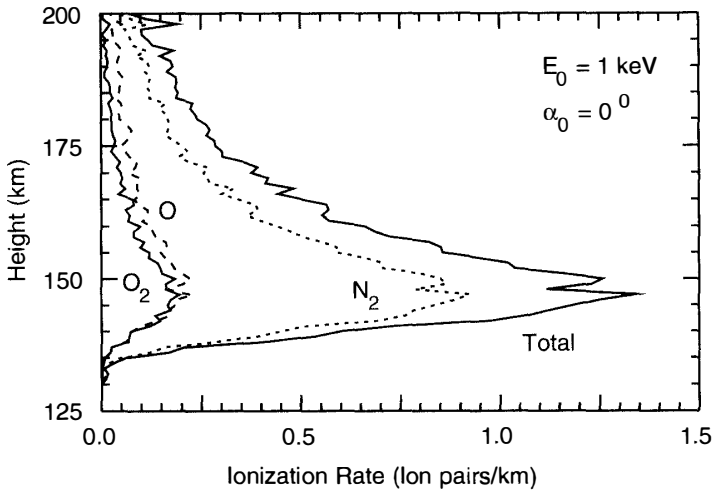

Fig. 1a. Ionization rates per primary electron of N_2 (shown by a dashed line with the character N_2), O (presented by a long dashed line with O), and O_2 (represented by a solid line with O_2) and the total ionization rate per primary electron (shown by a solid line with "Total") as a function of height at the initial electron energy E_0= 1 keV and the initial pitch angle α_0=0°.

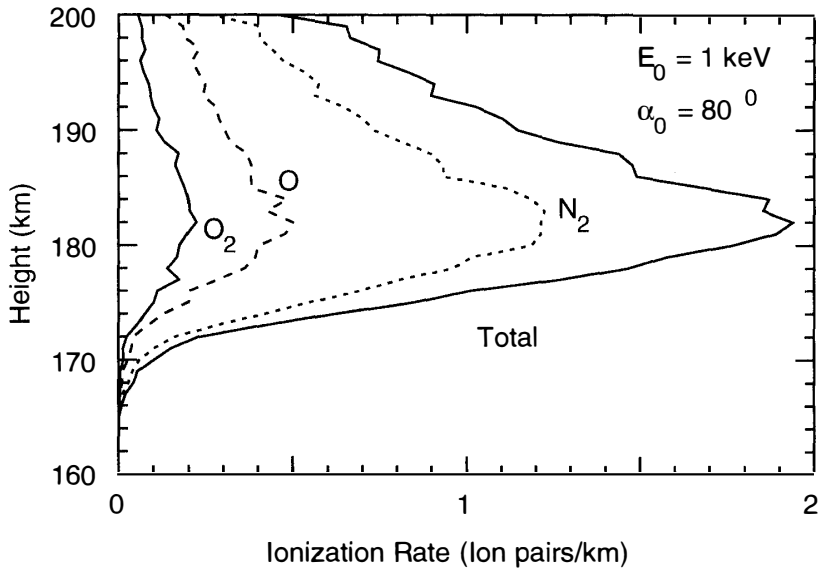

Fig. 1b. The same as Fig. 1a except for the initial pitch angle α_0=80°.

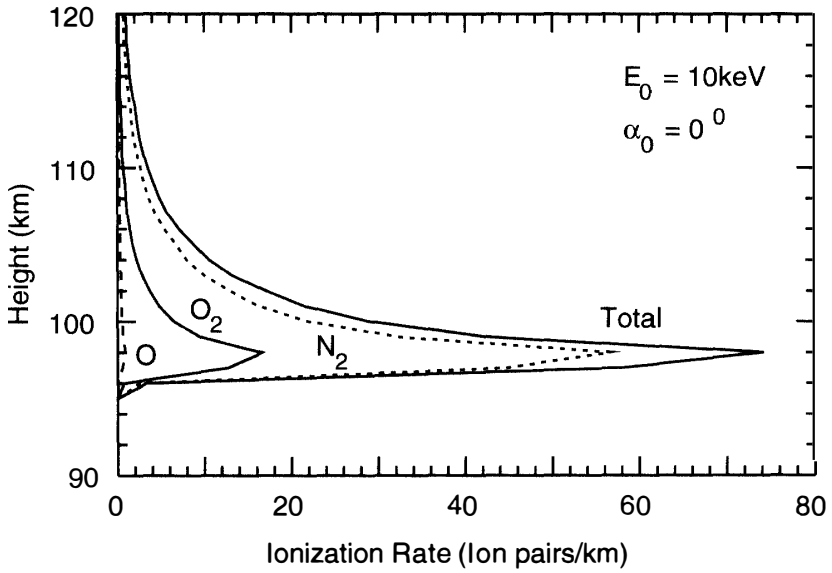

Fig. 2a. The same as Fig. 1a except for the initial electron energy E_0=10 keV.

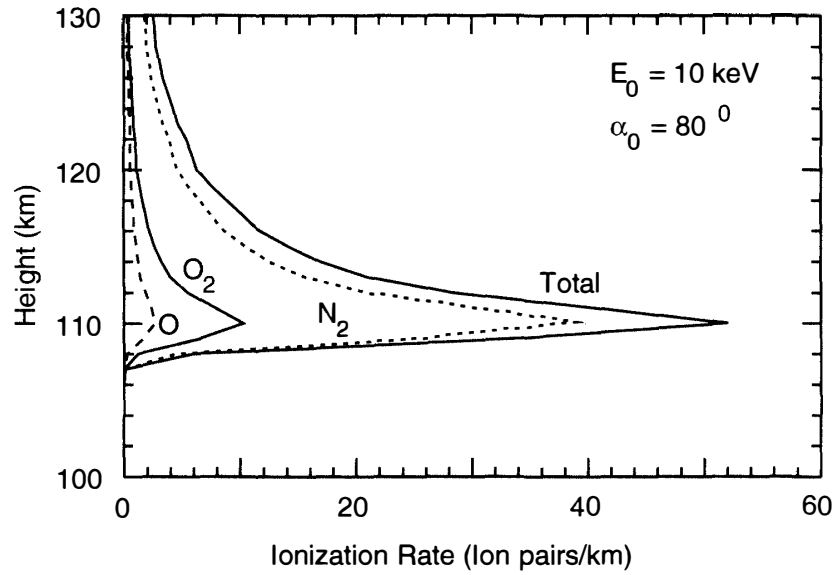

Fig. 2b. The same as Fig. 2a except for the initial pitch angle α_0=80°.

monitor the two-dimensional panchromatic auroral emission; the photometer (PHO) to measure an absolute intensity of λ 427.8 nm emission; the electron spectrum analyzer (ESP) to measure electron energy spectra with three pitch angles, *i.e.*, down-ward, trapped and up-ward; a number of electrons (NEL) by a swept-frequency impedance probe and a Langmuir probe; and a temperature of electron (TEL) by a resonance probe. The sounding rocket S-310JA-8 was launched at 1927:01 (UT) northward in the geomagnetic meridian (azimuth of 313°). An apogee was a height of 202 km and a total flight period was 429 s. The planetary magnetic three-hour-range indices, *Kp*, was 8, that is, at the substorm expansion phase. The rocket traversed the different

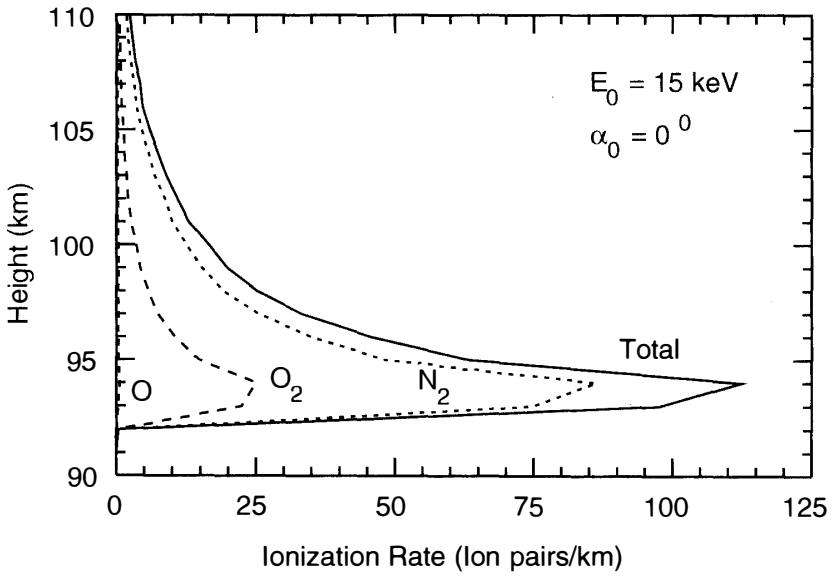

Fig. 3a. The same as Fig. 1a except for the initial electron energy E_0=15 keV.

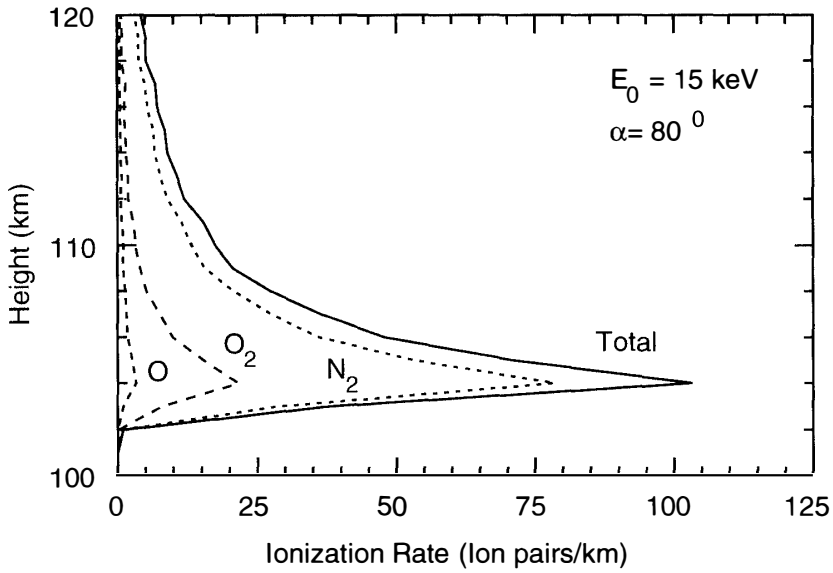

Fig. 3b. The same as Fig. 3a except for the initial pitch angle α_0=80°.

magnetic field lines during its flight. Therefore, the electron density profile observed by this rocket experiment was a profile of the *in-situ* electron density along the rocket trajectory for about 7 min, and was not a snapshot of the one along the geomagnetic field line. On the other hand, the theoretical electron density distribution shown below is the one along the field line, because the electron energy spectra observed at around the apogee were used in our calculations. The details of this rocket experiment were described by EJIRI *et al.* (1988c).

A previous study (see ONDA *et al.*, 1992) showed that secondary electrons having energy below 100 eV produced by the ionization were abundant in number. In

order to understand how far these secondary electrons can travel around, the mean free path of the electron was estimated to be from about 1300 m for the energy of 100 eV to 980 m for 30 eV at the altitude of 200 km, from 220 m for 100 eV to 160 m for 30 eV at 150 km, and from 30 m for 100 eV to 20 m for 30 eV at 120 km. If we take into account these values of the mean free path of the electron, the secondary electrons produced through the ionization of the atmospheric constituents are regarded as to be immediately thermalized at the height of ionization. Therefore, the altitude distribution of the total ionization rate can give the production rate of ther-

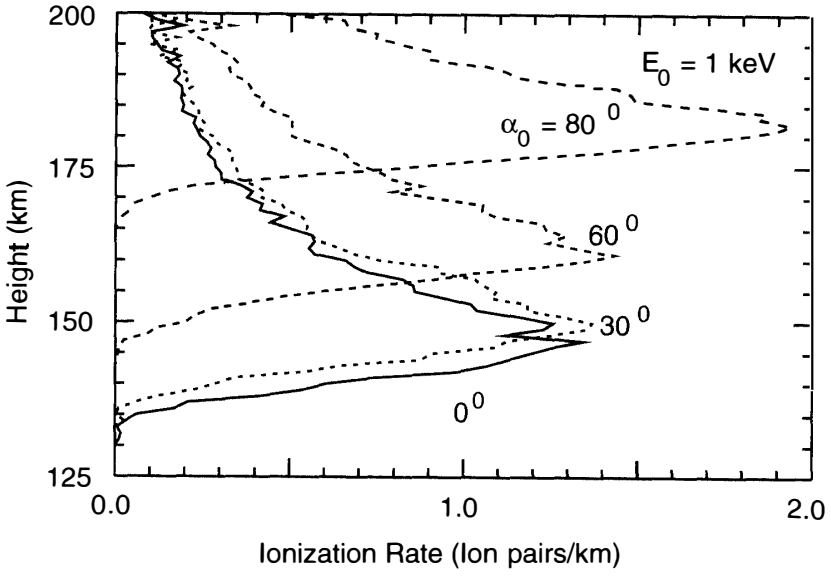

Fig. 4a. Altitude dependence of the total ionization rate per primary electron calculated for the pitch angles of 0°, 30°, 60° and 80° at the initial electron energy E_0=1 keV.

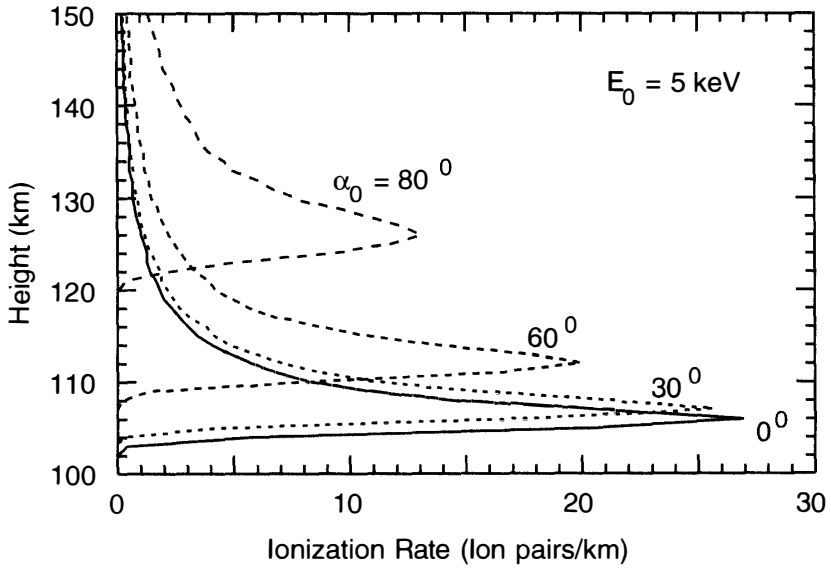

Fig. 4b. The same as Fig. 4a except for the initial electron energy E_0=5 keV.

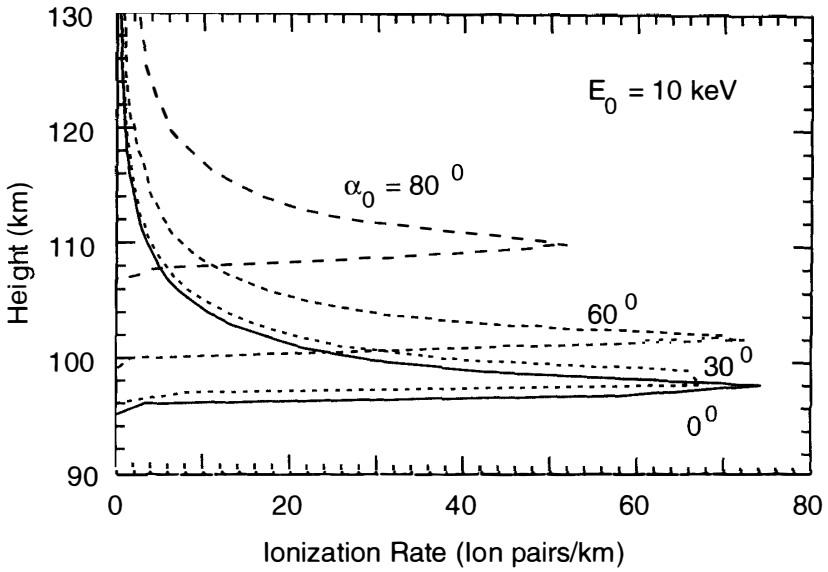

Fig. 4c. The same as Fig. 4a except for the initial electron energy E_0=10 keV.

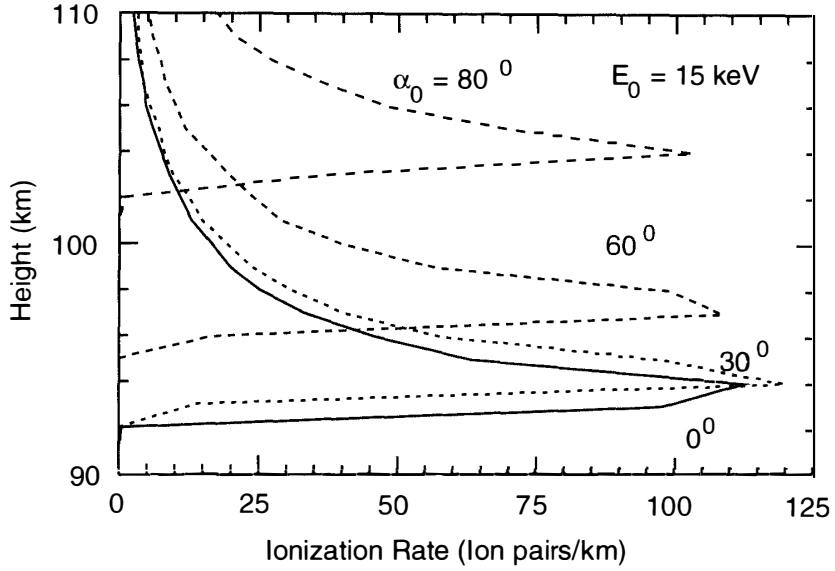

Fig. 4d. The same as Fig. 4a except for the initial electron energy E_0=15 keV.

mal electrons.

In order to estimate the absolute production rate of thermal electrons, the altitude distribution of the total ionization rate $I(\alpha, h, E)$ per primary electron was integrated over the pitch angles as follows: $I(h, E)=2\pi \int_0^{\pi/2} I(\alpha, h, E) \sin\alpha \, d\alpha = 2\pi \int_0^1 I(z, h, E) \, dz \simeq \frac{\pi}{2} [I(z=0, h, E)+I(z=\frac{1}{2}, h, E)+I(z=\frac{\sqrt{3}}{2}, h, E)+I(z\simeq 1, h, E)]$. Here, we assumed that the pitch angle distribution was uniform in the range of $[0, \pi/2]$. The absolute altitude distribution of the production rate of thermal electrons $Q_e(h)$ was calculated by integrating the altitude distribution of the total ionization rate multiplied by the electron differential flux over the initial energy of precipitating electrons such

as $\int_{E_{min}}^{E_{max}} j(E)\ I(h, E)\ dE$ particles $cm^{-3}s^{-1}$, where $j(E)$ is the electron differential flux measured by the sounding rocket experiment. The electron differential flux $j(E)$ at the time T=X+189, X+195, X+201, X+208, or X+226 s is presented in Fig. 5 as a function of energy in the range from 16 eV to 14.4 keV. The flux for the energy

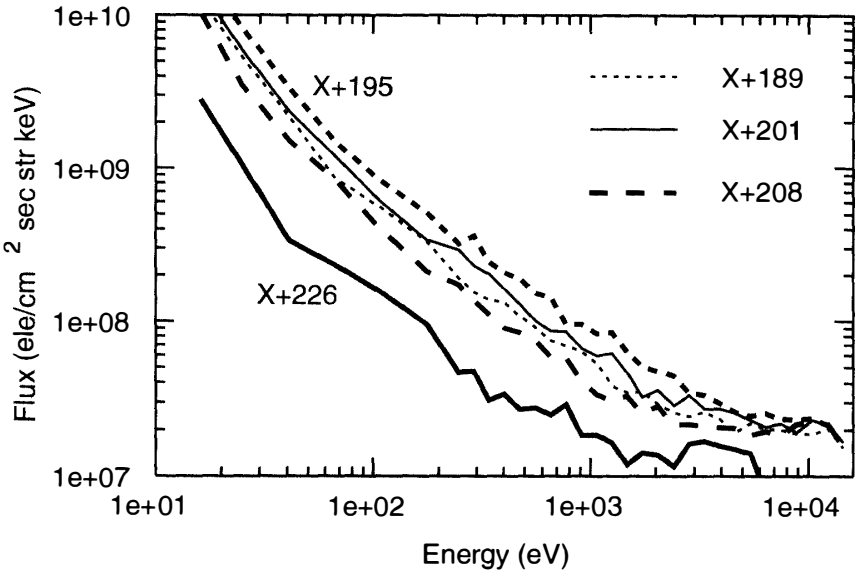

Fig. 5. Electron differential flux as a function of the electron energy observed by the sounding rocket S-310JA-8 at Syowa Station on April 4, 1984. The thin dotted line is the value at the time X+189 s, the thick broken line the one at X+195 s, the solid line the one at X+201 s, the thick long broken line the one at X+208 s, and the thick solid line the one at X+226 s.

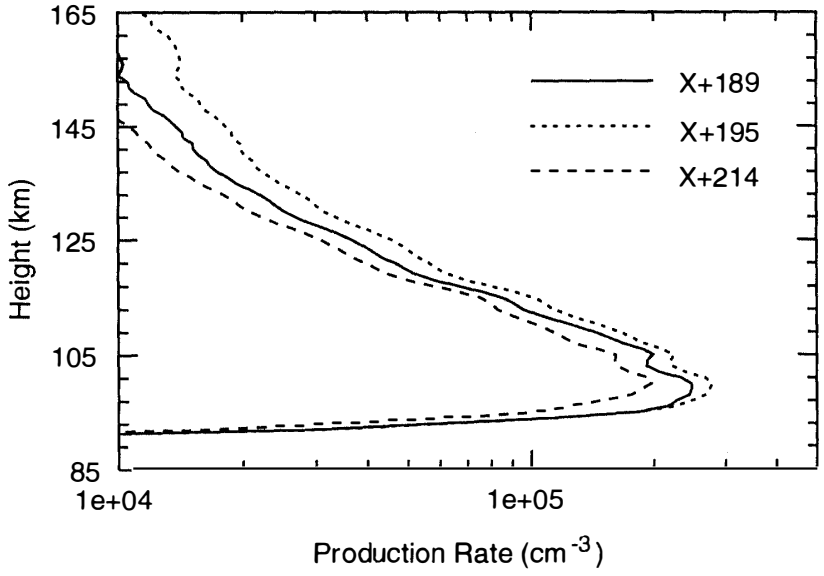

Fig. 6. Altitude dependence of the production rates of thermal electrons calculated at X+189 (shown by a solid line), X+195 (represented by a dashed line) and X+214 (presented by a long dashed line) s.

higher than 14.4 keV was obtained by an extrapolation with using a formula $j(E)=j(E=12.25\ \text{keV})\ (E(\text{in keV})/12.25)^{-5.2}$, which was deduced from the high energy part of the energy flux observed at the time T=X+220 s. We extended this calculation up to 18 keV for the initial energy of electron. The absolute value of the production rate of thermal electrons $Q_e(h)$ is displayed in Fig. 6 as a function of height. Since the electron differential flux drops rapidly beyond 18 keV as can be understood from the extrapolation formula shown above and the peak height of the ionization rate becomes lower than 90 km as the initial electron energy is increased above 18 keV, the contribution from the energy region above 19 keV to the production rate of thermal electrons was estimated to be negligible in the height profile of electron density above 90 km.

The value of an effective recombination coefficient α_{eff} depends on electron temperatures, which were about 500 K at the height of 100 km and 700 K at 150 km, and increased rapidly to 1750 K at 200 km as measured with TEL (EJIRI *et al.*, 1988c). It is not established yet what is the reliable value of α_{eff} as a function of height in the range from 100 km to 200 km. Here, we took tentatively $\alpha_{\text{eff}}=(2\sim3)\times10^{-7}\ \text{cm}^3\text{s}^{-1}$ estimated by OSEPIAN and KIRKWOOD (1996) at the height around 100 km.

A height profile of the absolute electron density was calculated by using a relation of $N_e(h)=(Q_e(h)/\alpha_{\text{eff}})^{1/2}$ under the assumption that the production and loss of thermal electrons were locally in equilibrium. The height profile of electron density thus estimated is compared in Fig. 7 with the value deduced from the sounding rocket experiment carried out by EJIRI *et al.* (1988c) as a function of time after launching the rocket. Theoretical results were obtained by using the value of effective recombination coefficient $\alpha_{\text{eff}}=3\times10^{-7}\ \text{cm}^3\text{s}^{-1}$ and the electron differential flux at three dif-

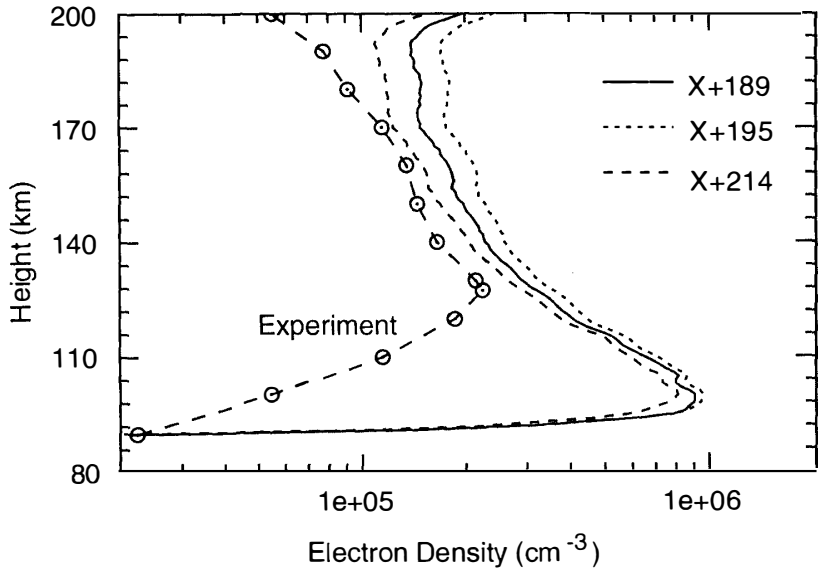

Fig. 7. Altitude dependence of the electron number density estimated by using an effective recombination rate of $\alpha_{\text{eff}}=3.0\times10^{-7}\ \text{cm}^3\text{s}^{-1}$ calculated at X+189 s (a solid line), X+195 s (a dashed line) and X+214 s (a long dashed line). The observed in-situ electron density is also shown by the circled data point.

ferent times of X+189 s, X+195 s, and X+214 s. The experimental values of the electron density were measured during the ascending phase of rocket. As can be seen from Fig. 7, the theoretical electron density agrees reasonably well with the experimental result in the range of the height from 125 km to 170 km.

Now we discuss a discrepancy between the peak height of the electron density measured by the rocket experiment and that obtained theoretically. Since the rocket traversed the different magnetic field lines during ascending phase, it is highly probable that the electron density measured at the height below 125 km is not related to the active aurora arcs, for which the electron differential flux was measured at around the apogee of the rocket. Although the theoretical electron density depends strongly on the value of effective recombination coefficient α_{eff}, the peak height of the electron density should be independent of the value of α_{eff}. The reason is that the height distribution of the production rate of thermal electrons and the peak height of electron density are determined by the electron differential flux measured by the rocket experiment. Since the electron differential flux extends in energy up to about 15 keV as can be understood from Fig. 5, the peak of the theoretical production rate of thermal electron attained a height of about 100 km as represented in Fig. 6. The ionization cross sections of N_2, O, and O_2 by the electron impact are measured with sufficient accuracy. Therefore, the theoretical ionization rates shown in Figs. 1–4 above are reasonably reliable. By considering these facts, the peak height of the theoretical thermal electron density is considered to be reasonably accurate compared with that measured by the rocket experiment.

Precipitating electrons having the energy below a few keV mainly contribute to the source of the thermal electrons at a height above 170 km. The magnitude of the electron differential flux at the energy below 1 keV is larger than the one at the energy above several keV by about 10 times. This is the reason why the theoretical electron density began to increase at a height above 170 km. But, the experimental result keeps decreasing in the electron density. We cannot understand this discrepancy between the experimental result and theoretical one.

In our calculation, we employed the value of $\alpha_{\text{eff}}=3\times10^{-7}$ cm^3s^{-1} irrespective of the height. Since the electron temperatures were changed from 500 K at the height of 100 km to 1750 K at 200 km, the value of α_{eff} should be decreased as the electron temperature rises. But, there is no data available for α_{eff} as a function of the height. Therefore, it is highly desirable for experimentalists to measure as many as possible electron densities in active auroras. Such experimental results should be useful to estimate the value of reliable effective recombination coefficient as a function of the height. It is also important to determine the contribution to the electron density from the background, which should be lessened to zero at midnight.

3.3. Photoemission rate of oxygen green line

The production of excited states of the atmospheric constituents N_2, O, and O_2 in this work is caused solely through collisions with precipitating electrons and the electrons produced by ionization. We consider the representative auroral emission from the excited states of $N_2^+(B^2\Sigma_u^+)$ and $O(^1S)$. The radiative lifetime of these excited states is known to be 60×10^{-9} s and 0.79 s, respectively. The excited state of $O(^1S)$

can be quenched by collision with N_2 and O_2 before emission of photons (see TAKAYANAGI 1984; STREIT *et al.*, 1976). In order to estimate the emission rate of the oxygen green line, we have taken into account collisions of these excited O atoms with N_2 and O_2 molecules under the neutral gas temperature in the altitude range of 80–200 km (see ONDA *et al.*, 1992, in detail). Since the rate coefficient for $O(^1S)+O_2 \rightarrow O(^3P)+O_2$ is much larger than that for $O(^1S)+N_2 \rightarrow O(^3P)+N_2$, O_2 molecules play an important role in quenching the excited state $O(^1S)$.

We first consider the emission rate of the oxygen green line at λ 557.7 nm per primary electron. The contribution to the emission rate from the electron impact is represented by a long dashed line in Figs. 8a–d at the initial electron energies $E_0=1$, 5, 10, and 15 keV, respectively. By taking into account a height profile of the number density of O_2 molecules, it is understood that the collisional quenching effect is small for this emission at the altitude above 110 km. This emission is predominantly caused by the secondary electrons as the previous studies of ONDA *et al.* (1992) and ONDA and ITIKAWA (1995) have shown. The emission rate shown by a long dashed line in Figs. 8a–d is weakly dependent on the initial energy of precipitating electrons. This weak energy dependence reflects the fact that $O(^1S)$ state is effectively excited through impact of secondary electrons.

It was pointed out by MEYER *et al.* (1969) and PARKINSON and ZIPE (1970) and has been investigated quantitatively by GATTINGER *et al.* (1985), GERDJIKOVA and SHEPHERD (1987), and SHEPHERD *et al.* (1995) that the major production process of $O(^1S)$ can be the following collision process:

$$N_2(A^3\Sigma_u^+)+O(^3P) \rightarrow N_2(X^1\Sigma_g^+)+O(^1S). \quad (1)$$

Since $N_2(A^3\Sigma_u^+)$ state was produced by collision of precipitating electrons with N_2 in the electronic ground state, its abundance can be calculated by our Monte Carlo method. Therefore, it is possible to estimate the production rate of $O(^1S)$ through this process, if the rate coefficient for this process is available. As pointed out by SHEPHERD *et al.* (1995), the value of this rate coefficient was experimentally determined by PIPER (1982) and reanalyzed by DE SOUZA *et al.* (1985) to be 2.1×10^{-11} cm^3s^{-1} at temperature of 298 K. We employed this value as the rate coefficient of the collision process eq. (1) in the following. The emission rate of the oxygen green line through this collision process was thus calculated and shown by a dashed line in Figs. 8a–d. As can be understood from these figures, the emission rate through this collision process is larger than that through electron collision by a factor of about 6 at $E_0=1$ keV, 30 at $E_0=5$ keV, 45 at $E_0=10$ keV, and 65 at $E_0=15$ keV, respectively.

Note that a large structure seen in Figs. 8a–d is caused by our numerical procedures, in which the initial pitch angles were taken to be 0°, 30°, 60°, and 80°. If we want to have a smooth curve for the emission rate, we have to execute the Monte Carlo calculations at much finer intervals of the pitch angle. Since a global height profile of the emission rate can be grasped from these figures, any further calculations are thought to be unnecessary.

The absolute emission rate of the green line was obtained by integrating the product of the height profile of the green line emission rate multiplied by the electron differential flux $j(E)$ over the initial energy of the precipitating electrons. The result is illustrated in Fig. 9. It is clearly seen that the collision process eq. (1) dominantly

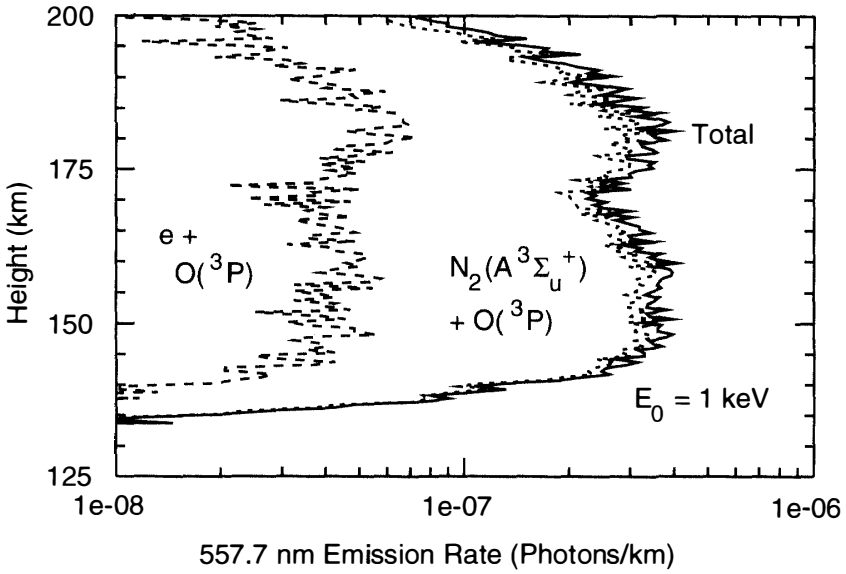

Fig. 8a. Altitude dependence of the 557.7 nm emission rates from $O(^1S)$ produced by the electron impact shown by a long dashed line with $e + O(^3P)$ and $N_2(A\,^3\Sigma_u^+)$ impact represented by a dashed line with $N_2(A^3\Sigma_u^+) + O(^3P)$ at the initial electron energy $E_0 = 1$ keV. The sum of the 557.7 nm emission rates calculated through both mechanisms is shown by a solid line with 'Total'.

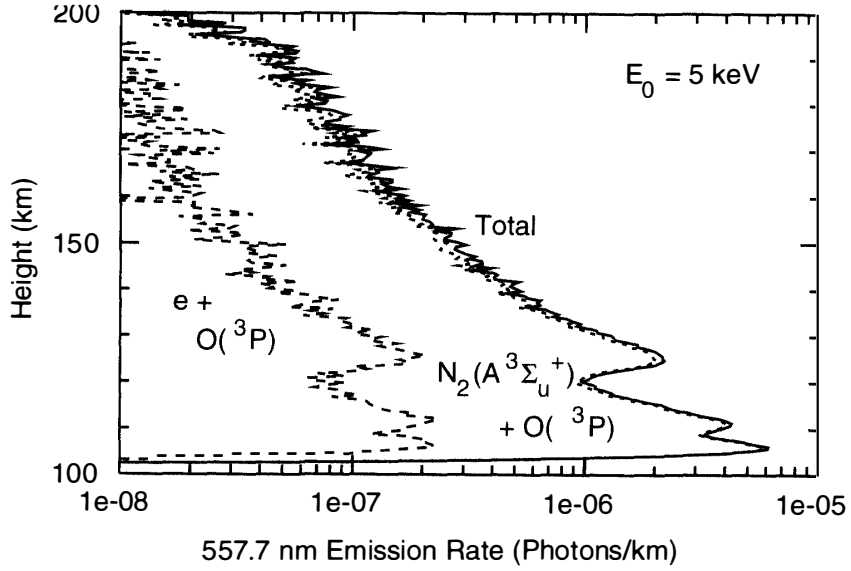

Fig. 8b. The same as Fig. 8a except for the initial electron energy at $E_0 = 5$ keV.

contributes to the emission rate of the green line. A similar height profile of the green line produced through this collision process was reported by SHEPHERD *et al.* (1995), who analyzed the experimental results obtained by experiments based on the Energy Budget Campaign 1980.

Since the production rate of $N_2^+(B^2\Sigma_u^+)$ per primary electron and the resultant emission rate for the first negative band system at λ 427.8 nm were reported by ONDA *et al.* (1997), only the height profile of the emission rate of this band system is pre-

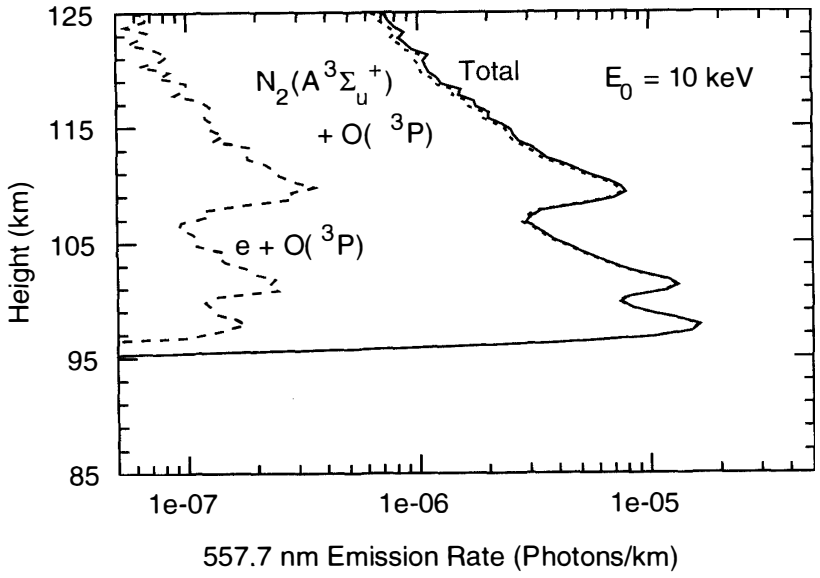

Fig. 8c. The same as Fig. 8a except for the initial electron energy at E_0=10 keV.

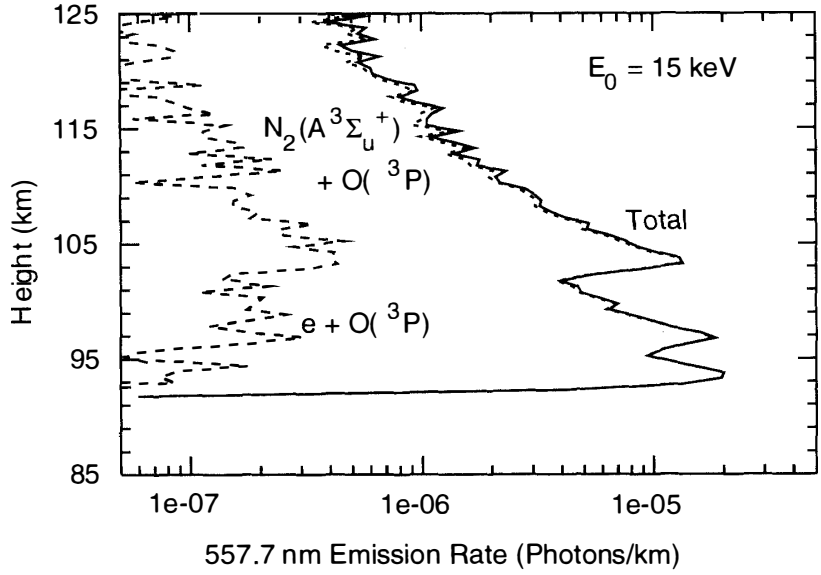

Fig. 8d. The same as Fig. 8a except for the initial electron energy at E_0=15 keV.

sented here. In Fig. 10, the absolute emission rate of the green line is compared with the one of the first negative band system of $N_2^+(B^2\Sigma_u^+)$. As can be understood from Fig. 9, the main contribution to the emission rate of the green line comes from $N_2(A\,^3\Sigma_u^+)$ impact. We employed the value of 2.1×10^{-11} cm^{3}s^{-1} as the rate coefficient of the collision process eq. (1). As pointed out by SHEPHERD *et al.* (1995), the value of this rate coefficient determined from aeronomical investigation was as small as $(0.3\text{–}0.78)\times10^{-11}$ cm^{3}s^{-1}. Thus, we took the value of 0.5×10^{-11} cm^{3}s^{-1} determined by GATTINGER *et al.* (1985) as an alternative value of this rate coefficient. In Fig. 10, a solid line represents the emission rate of the green line calculated by using this

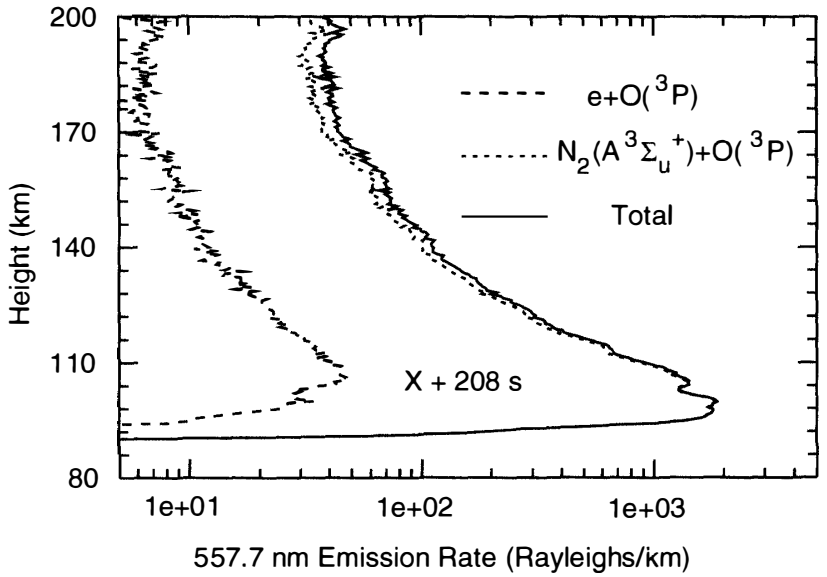

Fig. 9. Height profile of the absolute 557.7 nm emission rates calculated at the time X+208 s. Contribution from the electron impact is shown by a long dashed line and the one from $N_2(A^3\Sigma_u^+)$ impact is represented by a dashed line and the total emission rate is presented by a solid line.

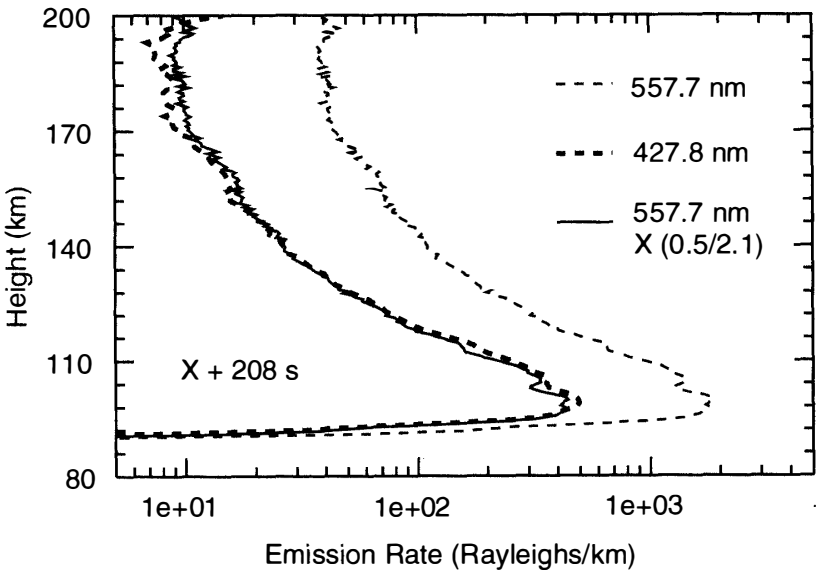

Fig. 10. Height profile of the absolute intensity of photon emissions at λ 427.8 nm in the first negative band system of $N_2^+(B^2\Sigma_u^+)$ shown by a thick dashed line and of the oxygen green line at 557.7 nm represented by a long dashed line, which was obtained by using the value 2.1×10^{-11} cm^3 s^{-1} as the rate coefficient for the collision process of $(A^3\Sigma_u^+)+O(^1S)$. A solid line shows the green line emission rate calculated by employing the value 0.5×10^{-11} cm^3s^{-1} instead of 2.1×10^{-11} cm^3s^{-1}. All emission profiles are calculated at the time of X+208 s.

smaller value of the rate coefficient of the collision process eq. (1).

It is important to measure the ratio of the emission intensity of the green line at λ 557.7 nm to that of the first negative band system at λ 427.8 nm. To measure simul-

taneously this intensity ratio, OKAMURA and EJIRI (1992) developed the imaging spectrometer which took snapshots (an exposure time of 3.2 s) of spectral apparent emission rate of aurora in a coordinate system of a wavelength from 300.3 nm to 732.5 nm and a spatial field of view of 72.6 degrees. Observations with this instrument were carried out at Syowa Station, Antarctica, in 1989 austral winter. The results showed various different spectral characteristics of aurora which, some cases, varied rapidly with a time, and the above ratio is, as a matter of course, also changing with auroral types. However, it is worth mentioning that the ratio observed in the middle of the auroral arc was 5.6 at the expansion phase (0001:07 UT, June 8, 1989). As can be understood from Fig. 10, the ratio of the emission intensity of λ 557.7 nm to that of λ 427.8 nm was about 3.8 at the height of 100 km, 4.2 at 140 km, and 5.0 at 180 km, respectively. Therefore, the result obtained by OKAMURA and EJIRI (1992) suggests that the value of rate coefficient can be slightly greater than 2.1×10^{-11} cm^3s^{-1} for the collision process eq. (1).

4. Concluding Remarks

We report here the results of simulation of collision processes of precipitating electrons with the atmospheric particles and emission processes in electron auroras observed by the sounding rocket experiment by using the Monte Carlo method. Our absolute electron density was reasonably in accord with the result deduced from the sounding rocket experiment at a height between 125 km and 170 km. The comparison in the thermal electron density clearly shows a discrepancy between the experiment and the theoretical results in the peak height of the electron density and the electron densities at a height above 170 km and below 125 km. One reason for this discrepancy below 125 km height comes from the fact that the measured electron density profile is not along the geomagnetic field line, and the horizontal distance between the rocket position at 125 km height and that at apogee was about 80 km. Thus, it is highly desirable to investigate the discrepancy further experimentally and theoretically. Specifically, the value of effective recombination coefficient must be experimentally determined as a function of height.

We also investigated the absolute intensity of the oxygen green line and of the first negative band system of nitrogen molecular ion $N_2^+(B^2\Sigma_u^+)$. If we employ the value of 2.1×10^{-11} cm^3s^{-1} determined in laboratories as the rate coefficient of the collision process $N^2(A^3\Sigma_u^+)+O(^3P) \rightarrow N_2(X^1\Sigma_g^+)+O(^1S)$, the absolute intensity of 557.7 nm emission line is much stronger than that of the first negative band system at λ 427.8 nm. But, if we take the value 0.5×10^{-11} cm^3s^{-1} determined by aeronomical investigation, the absolute intensity of the green line is very close to the one of the first negative band system. Therefore, it is crucially important to measure the ratio of intensity of 557.7 nm emission line to that of 427.8 nm band emission in electron auroras.

Acknowledgments

This work is one of the cooperative projects of National Institute of Polar Research

(NIPR) and Institute of Space and Astronautical Science (ISAS). The rocket experiment was performed by the 25th Japanese Antarctic Research Expedition (JARE). Numerical calculations have been done with the FACOM VPP-500 at the Computer Center, ISAS. One of the authors (K. O.) expresses his sincere thanks for the computer budget available at the Center for Planning and Information Systems in ISAS.

References

BANKS, P. M., CHAPPELL, C. R. and NAGY, A. F. (1974): A new model for the interaction of auroral electrons with the atmosphere: Spectral degradation, backscatter, optical emission, and ionization. J. Geophys. Res., **79**, 1459–1470.

BERGER, M. J., SELTZER, S. M. and MAEDA, K. (1970): Energy deposition by auroral electrons in the atmosphere. J. Atmos. Terr. Phys., **32**, 1015–1045.

CICERONE, R. J. and BOWHILL, S. A. (1971): Photoelectron fluxes in the ionosphere computed by a Monte Carlo method. J. Geophys. Res., **76**, 8299–8317.

DE SOUZA, A. R., GOUSSET, G., TOUZEAU, M. and KHIET, T. (1985): Note on the determination of the efficiency of the reaction $N_2(A^3\Sigma)+O(^3P)\rightarrow N_2+O(^1S)$. J. Phys. B: At. Mol. Phys., **18**, L661–L666.

DOERING, J. P. (1992): Absolute differential and integral electron excitation cross sections for atomic oxygen. 9. Improved cross section for the $^3P \rightarrow {}^1D$ transitions from 4.0 to 30 eV. J. Geophys. Res., **97**, 19531–19534.

DOERING, J. P. and GULCICEK, E.E. (1989): Absolute differential and integral electron excitation cross sections for atomic oxygen. 7. The $^3P\rightarrow{}^1D$ and $^3P\rightarrow{}^1S$ transitions from 4.0 to 30 eV. J. Geophys. Res., **94**, 1541–1547.

EJIRI, M. (1988): Results of sounding rocket experiments at Syowa Station, Antarctica, 1984, Upper Atmosphere Division, National Institute of Polar Research, Jpn.

EJIRI, M. and OBAYASHI, T. (1970): Measurement of ionosphere by the gyro-plasma probe. Rep. Ionos. Space Res. Jpn., **24**. 1–12.

EJIRI, M., FUKUNISHI, H., ONO, T., YAMAGISHI, H., HIRASAWA, T., KIMURA, I. and OGUTI, T. (1988a): Auroral phenomena observed by the sounding rockets S-310JA-8 to -12 at Syowa Station, Antarctica. J. Geomagn. Geoelectr., **40**, 763–781.

EJIRI, M., ONO, T., OGUTI, T., YAJIMA, N., KAMEDA, Y., HAMADA, H., and KOMATSU, K. (1988b): Visible auroral television camera for the sounding rockets S-310JA-8, -9, and -10. J. Geomagn. Geoelectr., **40**, 783–797.

EJIRI, M., ONO, T., HIRASAWA, T. and OGUTI, T. (1988c): Auroral images and particle precipitations observed by S-310JA-8, -9, and -10 at Syowa Station. J. Geomagn. Geoelectr., **40**, 799–815.

GATTINGER, R. L., HARRIS, F. R. and VALLANSE JONES, A. (1985): The height, spectrum and mechanism of type B red aurora as its bearing on the excitation of $O(^1S)$ in aurora. Planet. Space Sci., **33**, 207–221.

GERDJIKOVA, M. D. and SHEPHERD, G. G. (1987): Evaluation of auroral 5577 A excitation processes using intercosmos Bulgaria-1300 measurements. J. Geophys. Res., **92**, 3367–3374.

HEDIN, A. E. (1983): A revised thermospheric model based on mass spectrometer and incoherent scatter data: MSIS-83. J. Geophys. Res., **88**, 10170–10188.

HEDIN, A. E. (1987): MSIS-86 thermospheric model. J. Geophys. Res., **92**, 4649–4662.

ITIKAWA, Y., HAYASHI, M., ICHIMURA, A., ONDA, K., SAKIMOTO, K., TAKAYANAGI, K., NAKAMURA, M., NISHIMURA, H. and TAKAYANAGI, T. (1986): Cross sections for collisions of electrons and photons with nitrogen molecules. J. Phys. Chem. Ref. Data, **15**, 985–1010.

ITIKAWA, Y., ICHIMURA, A., ONDA, K., SAKIMOTO, K., TAKAYANAGI, K., HATANO, Y., HAYASHI, M., NISHIMURA, H. and TSURUBUCHI, S. (1989): Cross sections for collisions of electrons and photons with oxygen molecules. J. Phys. Chem. Ref. Data, **18**, 23–42.

ITIKAWA, Y. and ICHIMURA, A. (1990): Cross sections for collisions of electrons and photons with atomic oxygen. J. Phys. Chem. Ref. Data, **19**, 637–651.

JACKMAN, C. H. and GREEN, A. E. S. (1979): Electron impact on atmospheric gases. 3. Spatial yield spec-

tra for N_2. J. Geophys. Res., **84**, 2715–2724.

LINK, R. (1992): Feautrier solution of the electron transport equation. J. Geophys. Res., **97**, 159–169.

MEYER, J. A., STETSER, D. W. and STEDMAN, D. H. (1969): Excitation of the auroral green line of atomic oxygen ($^3P \dashrightarrow {}^1S$) by $N_2(A^3\Sigma_u^+)$. Astrophys. J., **157**, 1023–1025.

OKAMURA, H. and EJIRI, M. (1992): A new imaging spectrometer for the auroral spectroscopic studies. J. Geomagn. Geoelectr., **44**, 193–205.

ONDA, K. and ITIKAWA, Y. (1995): Simulation of particle precipitation and emission processes in electron auroras. Proc. NIPR Symp. Upper Atmos. Phys., **8**, 24–36.

ONDA, K., HAYASHI, M. and TAKAYANAGI, K. (1992): Monte Carlo calculation of ionization and excitation rates in electron aurora. ISAS Report, **645**, 1–38.

ONDA, K., MIYAOKA, H., ITIKAWA, Y. and EJIRI, M. (1997): Simulation of auroral photo-emission rate of the first negative band system of N_2^+ at λ 427.8 nm using measured electron differential number flux observed by the sounding rocket. Proc. NIPR Symp. Upper Atmos. Phys., **10**, 1–15.

OPAL, C. B., PETERSON, W. K. and BEATY, E. C. (1971): Measurements of secondary-electron spectra produced by electron impact ionization of a number of simple gases. J. Chem. Phys., **55**, 4100–4106.

OPAL, C. B., BEATY, E .C. and PETERSON, W. K. (1972): Tables of secondary-electron production cross sections. Atomic Data, **4**, 209–253.

OSEPIAN, A. and KIRKWOOD, S. (1996): High-energy electron fluxes derived from EISCAT electron density profiles. J. Atmos. Terr. Phys. **58**, 479–487.

OYA, H. (1965): Effect of resonances on the admittance of an RF plasma probe surrounded by an ion sheath. Rep. Ionos. Space Res. Jpn., **19**, 243–271.

PARKINSON, T. D. and ZIPF, E. C. (1970): Energy transfer from $N_2(A^3\Sigma_u^+)$ as a source of $O(^1S)$ in the aurora. Planet. Space Sci., **18**, 895–900.

PIPER, L. G. (1982): The excitation of $O(^1S)$ in the reaction between $N_2(A^3\Sigma_u^+)$ and $O(^3P)$. J. Chem. Phys., **77**, 2373–2377.

REES, M. H. (1963): Auroral ionization and excitation by incident energetic electrons. Planet. Space Sci., **11**, 1209–1218.

REES, M. H. (1969): Auroral electrons. Space Sci. Rev., **10**, 413–441.

REES, M. H. and ROBLE, R. G.(1975): Observations and theory of the formation of stable auroral red arcs. Rev. Geophys. Space Phys., **13**, 201–242.

REES, M. H. (1987): Modeling of the heating and ionizing of the polar thermosphere by magnetospheric electron and ion precipitation. Phys. Scrip., **T18**, 249–255.

SERGIENKO, T. I. and IVANOV, V. E. (1993): A new approach to calculate the excitation of atmospheric gases by auroral electron impact. Ann. Geophys., **11**, 717–727.

SHEPHERD, M. G., MCCONNELL, J. C., TOBISKA, W. K., GLADSTONE, G.R., CHARABARTI, S. and SCHMIDTKE, G. (1995): Inference of atomic oxygen concentration from remote sensing of optical aurora. J. Geophys. Res., **100**, 17415–17428.

SOLOMON, S. C. (1991): Optical aeronomy. Rev. Geophys. Suppl., **29**, 1089–1109.

SOLOMON, S. C. (1993): Auroral electron transport using the Monte Carlo method. Geophys. Res. Lett., **20**, 185–188.

SOLOMON, S. C., HAYS, P. B. and ABREU, V. J. (1988): The auroral 6300 A emission: Observation and modeling. J. Geophys. Res., **93**, 9867–9882.

STREIT, G. E., HOWARD, C. J., SCHMELTEKOPF, A. L., DAVIDSON. J. A., and SCHIFF, H. I. (1976): Temperature dependence of O (^1D) rate constants for reactions with O_2, N_2, CO_2, O_3, and H_2O. J. Chem. Phys., **65**, 4761–4764.

STRICKLAND, D. J., BOOK, D. L., COFFEY, T. P. and FEDDER, J. A. (1976): Transport equation techniques for the deposition of auroral electrons. J. Geophys. Res., **81**, 2755–2764.

TAKAYANAGI, K. (1984): A numerical study of artificial electron aurora experiment. ISAS Report, **611**, 1–32.

TORR, M. R. and TORR, D. G. (1982): The role of metastable species in the thermosphere. Rev. Geophys. Space Phys., **20**, 91–144.

YUROVA, I. Y. and IVANOV, V. E. (1989): Electron cross sections of atmospheric gases. Leningrad, Nauka (in Russian).

(Received March 23, 1997; Revised manuscript accepted July 23, 1997)